Ceramics International 30 (2004) 1283–1287

CERAMICS INTERNATIONAL

www.elsevier.com/locate/ceramint

Dielectric properties and microstructure of magnesium-doped $Ba_{1+k}(Ti_{1-x}Ca_x)O_{3-x+k}$ ceramics

Yanxia Li*, Xi Yao, Liangying Zhang

Functional Materials Research Laboratory, Tongji University, Shanghai 200092, China

Received 4 December 2003; received in revised form 18 December 2003; accepted 22 December 2003

Abstract

The dielectric properties and microstructure of magnesium-doped $Ba_{1+k}(Ti_{1-x}Ca_x)O_{3-x+k}$ ceramics have been investigated. When $Ba_{1+k}(Ti_{1-x}Ca_x)O_{3-x+k}$ ceramics, $0 \leq x \leq 0.02$, $0 \leq k \leq 0.01$, sintered in pure nitrogen, it behaves as undoped barium titanate. In this study, microstructure, electrical resistivity and dielectric characteristics of magnesium-doped $Ba_{1+k}(Ti_{1-x}Ca_x)O_{3-x+k}$ ceramics with various k and x value and magnesium concentration are studied systematically. Moreover, the effects of Ba/Ti ratio on microstructure and dielectric properties were studied. The results show that Magnesium-doped $Ba_{1+k}(Ti_{1-x}Ca_x)O_{3-x+k}$ was more difficult to sinter than ceramic $Ba_{1+k}(Ti_{1-x}Ca_x)O_{3-x+k}$. Ca and Mg co-doped $BaTiO_3$ has the poorest electrical resistivity properties compared to Ca- or Mg-doped $BaTiO_3$. When temperature is higher than 100 °C, the curve of temperature dependence of dielectric loss warps upwards markedly, which is caused by migration of oxygen vacancies. Ba/Ti ratio had an important impact on the Curie temperature.

Keywords: B. Microstructure; C. Dielectric properties; D. Barium titanate; Electrical resistivity; Base metal electrode

1. Introduction

Since the discovery of barium titanate ($BaTiO_3$) in the early 1940s, there has been a continuous development of using it in new industrial and commercial applications [1]. With the tendency towards miniaturization of electronic devices, multilayer ceramic capacitors (MLCCs) require higher volume efficiency [2–4]. This means that the dielectric becomes thinner and the number of internal electrode layer increases. Recently MLCCs with internal electrodes made of a base metal such as Ni have been developed in an effort to reduce costs [5–9].

A Ni internal electrode is easily oxidized during firing under ambient conditions. Therefore, dielectric and internal electrode cofiring should be carried out in a reducing atmosphere. However, barium titanate ceramics tend to become semiconducting after being heated in atmosphere of low O_2 content [5–7,10]. The increase in conductivity has been explained by the formation of oxygen vacancies and the accompanying reduction of titanium to trivalent state, which can be compensated by incorporating a small amount of trivalent or divalent dopant on titanium sites [11,12].

According to the study on defect chemistry of barium titanate [9,11,13–15], A/B ratio has an important influence on sites-occupancy for the dopant ions. When A/B ratio > 1, the dopant ions tend to be on the B-sites [7,12,14].

One of the principal problems of variable valence acceptors is the valence instability at a change of the oxygen partial pressure during heat treatment of MLCCs. For this reason manufactures of BME-MLCCs make use of calcium or magnesium ions on Ti-sites, which have been reported as being strong acceptors [12]. Chan et al. found that Ca^{2+}-ions which are well known as A-sites substituents may also enter the B-sites of $BaTiO_3$. In the case of BaO-excess, a certain number of Ca^{2+}-ions is shifted from the Ba- to the Ti-sites [15]. Zhuang et al. observed a lowering of the Curie point, T_c, at the incorporation of $[Ca_{Ti}^{2+}]''$ in $BaTiO_3$ [14]. Zhang et. al. reported a maximum solubility of ≅5% $[Ca_{Ti}^{2+}]''$ in $BaTiO_3$ [13]. Kishi et al. [16] and Nagai et al. [17] reported that Mg ions incorporated into Ti sites, and the solubility limit for $[Mg_{Ti}^{2+}]''$ is about 2.0 mol%.

In this paper, with control of A/B ratio ≥ 1, samples with dopant calcium, magnesium, combination of calcium and

---

* Corresponding author. Fax: +86-21-6598-5179.
E-mail address: liyanxia@fmrl.ac.cn (Y. Li).

0272-8842/$30.00 © 2004 Elsevier Ltd and Techna Group S.r.l. All rights reserved.
doi:10.1016/j.ceramint.2003.12.036

magnesium on Ti-sites were prepared. Sintering atmosphere was pure nitrogen. The microstructure, dielectric properties and insulation performance were studied.

2. Experimental procedure

Formulations of samples were prepared according to Table 1. Sample preparation was performed by conventional powder processing method, including ball-milling, drying, uniaxially pressing, and sintering in pure nitrogen. The starting materials were hydrothermally synthesized $BaTiO_3$ and highly pure oxides (Reagent grade), $CaCO_3$, $(MgCO_3)_4·Mg(OH)_2·5H_2O$. Before mixing with the dopants, the hydrothermal $BaTiO_3$ was calcinated at 1000 °C to remove water and defects within it. The oxides dopants and the calcined hydrothermal $BaTiO_3$ were mixed by wet ball milling using deionized water and ZrO_2 balls (Ø 3 mm), then fired at 950 °C for 2 h to promote the diffusion of dopants. The calcined powders were then uniaxially pressed into disks with 10 mm in diameter and 1 mm in thickness. And then sintered in pure nitrogen at various temperatures. After sintering, silver electrode was coated on both sides of specimens for electrical measurements. Then, the samples with silver electrode were calcined at 520 °C in air. Microstructures of ceramics were studied on

Table 1
Compositions and densities of samples

Sample	Composition	Density
BTCa1	$Ba_{1.005}(Ti_{0.99}Ca_{0.01})O_{2.995}$	5.807
BTCa2	$Ba_{1.01}(Ti_{0.99}Ca_{0.01})O_3$	5.953
BTCa3	$Ba_{1.005}(Ti_{0.98}Ca_{0.02})O_{2.985}$	5.592
BTCa4	$Ba_{1.01}(Ti_{0.98}Ca_{0.02})O_{2.99}$	5.793
BTCa5	$Ba(Ti_{0.99}Ca_{0.01})O_{2.99}$	5.721
BTCa6	$Ba(Ti_{0.98}Ca_{0.02})O_{2.98}$	5.343
BTMg1	$Ba_{1.005}(Ti_{0.99}Mg_{0.01})O_{2.995}$	
BTMg2	$Ba_{1.01}(Ti_{0.99}Mg_{0.01})O_3$	
BTMg3	$Ba_{1.005}(Ti_{0.98}Mg_{0.02})O_{2.985}$	
BTMg4	$Ba_{1.01}(Ti_{0.98}Mg_{0.02})O_{2.99}$	
BCM1	$Ba_{1.005}(Ti_{0.985}Ca_{0.01}Mg_{0.005})O_{2.99}$	5.684
BCM2	$Ba_{1.01}(Ti_{0.985}Ca_{0.01}Mg_{0.005})O_{2.995}$	5.604
BCM3	$Ba_{1.005}(Ti_{0.98}Ca_{0.01}Mg_{0.01})O_{2.985}$	5.510
BCM4	$Ba_{1.01}(Ti_{0.98}Ca_{0.01}Mg_{0.01})O_{2.99}$	5.311

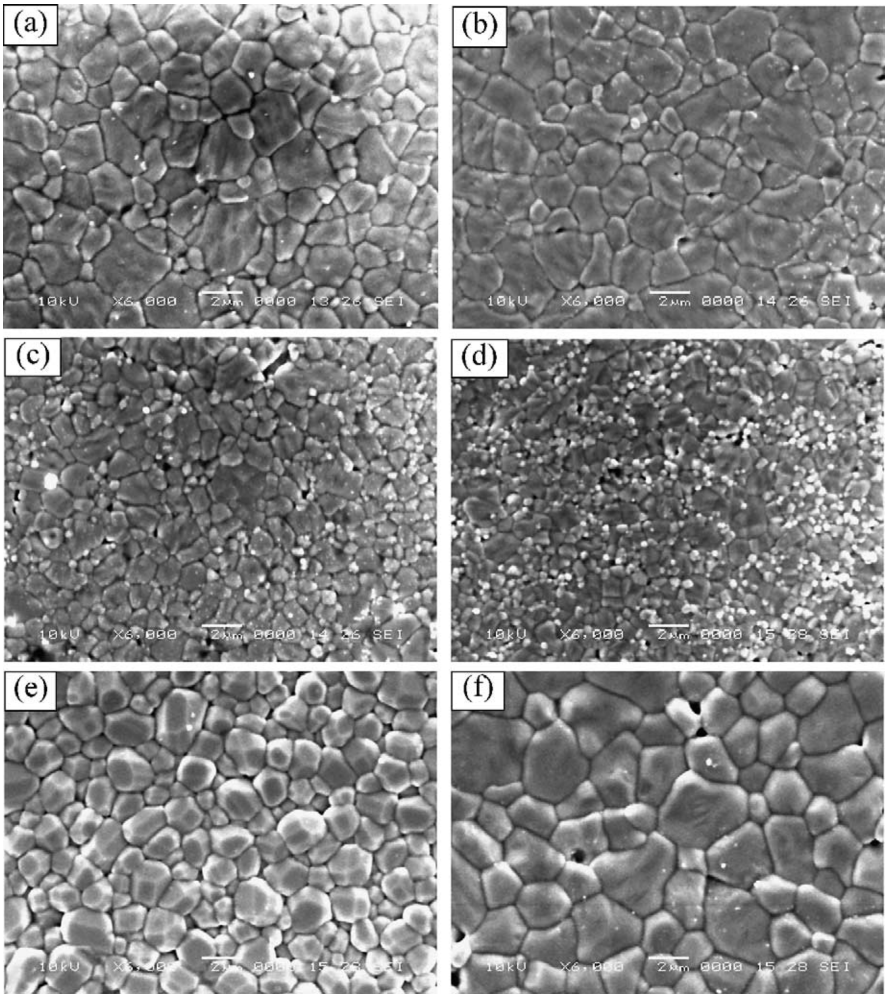

Fig. 1. SEM morphology of as-fired ceramics sintered at 1250 °C with a soak time 2 h in pure nitrogen: (a) BTCa1; (b) BTCa1; (c) BTCa3; (d) BTCa4; (e) BTCa5; (f) BTCa6.

the as-fired surfaces of the sintered ceramics using SEM (JEOL 5510LV) with an accelerating voltage of 10 kV.

Dielectric properties of sintered disk were measured from −60 to 160 °C with an impedance analyzer LCR (HP 4284A) at frequency of 1 kHz and oscillation level of 1 V rms. The heating rate was 2 °C/min and the accuracy was 0.1 °C.

After sintering, the apparent densities of samples were determined by the Archimedes method. Insulation resistivities were investigated by means of a high resistance meter (Keithley 6517A) using alternating polarity resistance test method. The alternating polarity resistance was designed to improve high resistance measurements and it was possible to eliminate the effects of background currents. The test voltage was 100 V.

3. Results and discussion

3.1. Theoretical analysis

The incorporation reaction of excess Ba and divalent cation in $BaTiO_3$ is:

$$BaO + RO \Rightarrow Ba_{Ba}^{\times} + R_{Ti}'' + 2O_{O}^{\times} + V_{O}^{\bullet\bullet} \qquad (1)$$

Using the kröger–Vink notation for point defects and R represents a +2 cation. Combine the corresponding mass action relation gives:

$$[R_{Ti}''] \times [V_{O}^{\bullet\bullet}] = Ks \qquad (2)$$

With doping concentration increasing, Eq. (1) reacts towards right, which would produce more oxygen vacancies and enlarge electrical conductivity. These were reflected in Fig. 3.

3.2. Sintering density

The sintering densities of BTCa1-6 and BCM1-4 were showed in Table 1. As can be seen from Table 1, densities of samples doped with Ca and Mg simultaneously were smaller than those of samples doped with Ca. when doping element was Ca, densities increased with Ba/Ti ratio increasing (doping concentration was fixed) and decreased with doping concentration increasing (Ba/Ti ratio was fixed). However, when doping elements were Ca and Mg simultaneously, densities decreased with Ba/Ti ratio increasing (doping concentration was fixed).

3.3. Microstructure development

Fig. 1 shows SEM morphology of as-fired ceramics sintered at 1250 °C with a soak time 2 h in pure nitrogen for samples doped with Ca. Compare (e), (a), (b) and (f), (c), (d), the doping concentration was fixed, as can be seen, with Ba/Ti ratio increasing, the size of ceramic becomes smaller, the holes and fissures become smaller and sparse, and the ceramic become denser. Compare (a), (c) and (b), (d) and (e), (f), Ba/Ti ratio was fixed, as can be seen, with doping concentration increasing, the holes and fissures become larger and more, and the ceramic become less dense. This is in agreement with the result of density measurement.

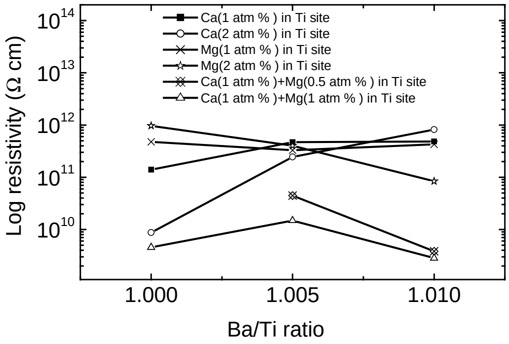

Fig. 2. Influence of Ba/Ti ratio and additive concentration on resistivity of Ca- and Mg-doped $BaTiO_3$.

3.4. Resistivity properties of as-fired ceramics

Electrical resistivity properties of as-fired ceramics $Ba_{1+k}(Ti_{1-x}Ca_x)O_{3-x+k}$ solid solutions measured at room temperature are shown in Fig. 2. Electrical resistivities of Ca substituted samples increased with Ba/Ti ratio increasing. However, electrical resistivities of Mg substituted samples

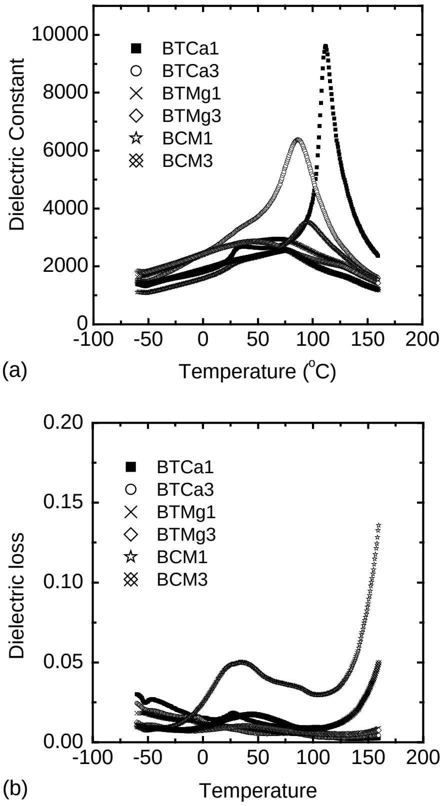

Fig. 3. Influence of doping elements and their concentration on the dielectric properties for samples Ba/Ti ratio equal to 1.005.

decreased with Ba/Ti ratio increasing, and electrical resistivities of Ca, Mg simultaneously substituted samples had a maximum when Ba/Ti ratio was equal to 1.005. As can be seen from Fig. 2, Electrical resistivity properties of Ca, Mg simultaneously substituted samples are inferior to those of Ca or Mg solely substituted samples. The difference is up to 1–2 orders of magnitude. When Ba/Ti ratio is equal to 1, Electrical resistivity properties for Ca substituted samples are superior to those for Mg substituted samples. This means that Ca enter into Ti-sites easier than Mg.

3.5. *Dielectric properties of as-fired ceramics*

When Ba/Ti ratio is equal to 1.005, influence of doping elements and their concentration on the dielectric properties is illustrated in Fig. 3. When Ba/Ti ratio is equal to 1.01, influence of doping elements and their concentration on the dielectric properties is shown in Fig. 4. As can be seen from Figs. 3 and 4, the dielectric properties of 1 at.% Ca additives on Ti-sites behaved as those of pure $BaTiO_3$, Ca ions on Ti-sites are strong dielectric inhibitors and T_c shifters. The Curie temperature decreased about 50 °C after doping concentration increased from 1 to 2 at.%. Mg ions on Ti-sites are stronger inhibitors. When doping concentration is 1 at.%, the dielectric constant is about 2000 without visible peaks. The dielectric properties of Ca, Mg simultaneously substituted samples resembled those of Ca-doped samples when Ca content is larger, and when Mg content is larger, the dielectric properties are similar to Mg-doped samples.

As can be seen from Figs. 3 and 4, when temperature is higher than 100 °C, the curve of temperature dependence of dielectric loss warped upwards markedly. Which is caused by the influence of leakage conductivity. In this experiment, the leakage conductivity was produced by migration of oxygen vacancies. Because temperature has an exponential influence on conductivity, leakage conductivity increases sharply in the range of high temperature. Polarization relaxation loss has a leading effect on dissipation factor in the range of low temperature, whereas, leakage conductivity increases sharply in exponential relation in the range of high temperature. The function of polarization relaxation loss is gradually weakened with conductivity increasing, until its effect disappears entirely. According to this, we can judge from Figs. 3 and 5, Ca and Mg simultaneously substituted samples have the largest conductivity, in other words, they have the smallest resistivity. The results matched well with electrical resistivity measurement.

Fig. 5 shows the influence of Ba/Ti ratio and dopant type on the dielectric properties for samples doped with acceptor (2 at.%) on Ti-site. In samples doped with Ca, the Curie temperature lowered with Ba/Ti ratio increasing. Whereas, in samples doped with Ca and Mg simultaneously, the Curie

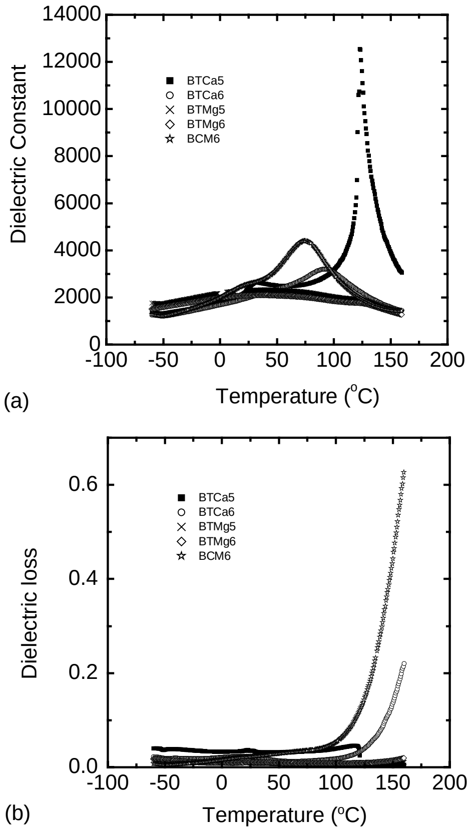

Fig. 4. Influence of doping elements and their concentration on the dielectric properties for samples Ba/Ti ratio equal to 1.01.

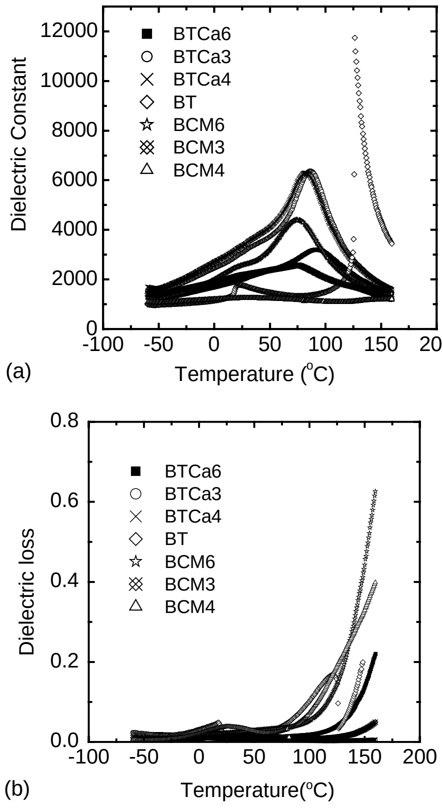

Fig. 5. Influence of Ba/Ti ratio and dopant type on the dielectric properties for samples acceptor (2 at.%) in Ti site.

temperature did not change on the whole. Ba/Ti ratio had an important effect on the dielectric constant, dielectric peaks broadened and the dielectric constant decreased intensively with Ba/Ti ratio augmentation.

4. Conclusions

Microstructure, Electrical resistivities and dielectric properties of magnesium-doped $Ba_{1+k}(Ti_{1-x}Ca_x)O_{3-x+k}$ have been studied in this paper.

1. Magnesium-doped $Ba_{1+k}(Ti_{1-x}Ca_x)O_{3-x+k}$ was more difficult to sinter than ceramic $Ba_{1+k}(Ti_{1-x}Ca_x)O_{3-x+k}$.
2. Compared to Ca- or Mg-doped $BaTiO_3$, Ca and Mg co-doped $BaTiO_3$ has the poorest electrical resistivity properties. The value for Ca and Mg co-doped $BaTiO_3$ is $10^{10}\,\Omega\,cm$, and the value for Ca- or Mg-doped $BaTiO_3$ is up to $10^{12}\,\Omega\,cm$.
3. The dielectric properties of 1 at.% Ca additives on Ti-sites behave as those of pure $BaTiO_3$. The dielectric properties of Ca and Mg co-doped samples behave between ca-doped $BaTiO_3$ and Mg-doped $BaTiO_3$.
4. When temperature is higher than 100 °C, the curve of temperature dependence of dielectric loss warps upwards markedly, which is caused by migration of oxygen vacancies. Ca and Mg co-doped $BaTiO_3$ have the largest conductivity.
5. Ba/Ti ratio had an important impact on the Curie temperature, for Ca-doped $BaTiO_3$, the Curie temperature was lowered with Ba/Ti ratio increasing. Whereas, for Ca and Mg co-doped $BaTiO_3$, the Curie temperature did not change basically.

Acknowledgements

This work was supported by the Ministry of Sciences and Technology of China through 973-project under grant 2002CB613302 and the university key studies project of Shanghai.

References

[1] A.J. Moulson, J.M. Herbert, Electroceramics: Materials, Properties and Applications, Chapman and Hall, London, 1990.
[2] Y. Okino, H. Shizuno, S. Kusuno, H. Kishi, Dielectric properties of rare-earth-oxide-doped $BaTiO_3$ ceramics fired in reducing atmosphere, Jpn. J. Appl. Phys. 33 (1994) 5393–5396.
[3] G. Arlt, D. Hennings, G. de with, Dielectric properties of fine-grain barium titanate ceramics, J. Appl. Phys. 58 (1985) 1619–1625.
[4] H. Konaka, H. Sano, T. konoike, K. Tomono, Microstructure control of $BaTiO_3$-based ceramics by the compositions, Key Eng. Mater. 181–182 (2000) 3–6.
[5] J.M. Herbert, High-permittivity ceramics sintered in hydrogen, Trans. Br. Ceram. Soc. 62 (1963) 645–658.
[6] I. Burn, G.H. Maher, High resistivity $BaTiO_3$ sintered in CO/CO_2 atmospheres, J. Mater. Sci. 10 (4) (1975) 633–640.
[7] P. Hansen, D. Hennings, H. Schreinemacher, High-k dielectric ceramics from donor/acceptor-codoped $(Ba_1(xCa_x)(Ti_{1-y}Zr_y)O_3$(BCTZ), J. Am. Ceram. Soc. 81 (5) (1998) 1369–1373.
[8] Y. Sakabe, Dielectric materials for base-metal multiplayer ceramic capacitors, Ceram. Bull. 66 (9) (1987) 1338–1341.
[9] J. Daniels, K.-H. Härdtl, D. Hennings, R. Wernicke, Defect chemistry and electrical conductivity of doped barium titanate ceramics, Philips Res. Rep. 31 (1976) 487–559.
[10] R. Waser, T. Baiatu, K.-H. Härdtl, DC electrical degradation of perovskite type titanates, J. Am. Ceram. Soc. 73 (6) (1990) 1645–1653.
[11] N.H. Chan, D.M. Smyth, Defect chemistry of donor-doped $BaTiO_3$, J. Am. Ceram. Soc. 67 (1984) 285–288.
[12] D. Hennings, H. Schreinemacher, Ca acceptors in dielectric ceramics sintered in reducing atmosphere, J. Eur. Ceram. Soc. 15 (1995) 795–800.
[13] X.W. Zhang, Y.H. Han, M. Lal, D.M. Smyth, Defect chemistry of $BaTiO_3$ with additions of $CaTiO_3$, J. Am. Ceram. Soc. 70 (1987) 100–103.
[14] Z.Q. Zhuang, M.P. Harmer, D.M. Smyth, R.E. Newnham, The effect of octahedrally-coordinated calcium on the ferroelectric transition of $BaTiO_3$, Mater. Res. Bull. 22 (1987) 1329–1335.
[15] N.H. Chan, M.P. Harmer, M. Lal, D.M. Smyth, Calcium site occupancy in $BaTiO_3$, Mater. Res. Soc. Symp. Proc. 31 (1984) 345–350.
[16] H. Kishi, Y. Okino, M. Honda, Y. Zguchi, M. Imaeda, Y. Takahashi, H. Ohsato, T. Okadu, The effect of MgO and rare-earth oxide on formation behavior of core–shell structure in $BaTiO_3$, Jpn. J. Appl. Phys. 36 (1997) 5954–5957.
[17] T. Nagai, K. Iijima, H.J. Hwang, M. Sando, T. Sekino, K. Nihara, Effect of MgO doping on the phase transformations of $BaTiO_3$, J. Am. Ceram. Soc. 83 (2000) 107–112.